https://doi.org/10.5194/tc-2021-398
Preprint. Discussion started: 14 February 2022

The Cryosphere Discussions
Open Access
EGU

Mechanism and effects of warming water in ice-covered Ngoring Lake of Qinghai-Tibet Plateau

Mengxiao Wang [1,2], Lijuan Wen [1*], Zhaoguo Li [1], Matti Leppäranta [3], Victor Stepanenko [4,5], Yixin Zhao [1,2], Ruijia Niu [1,2], Liuyiyi Yang [1,2] and Georgiy Kirillin [6]

[1] Key Laboratory of Land Surface Process and Climate Change in Cold and Arid Regions, Northwest Institute of Eco-Environment and Resources, Chinese Academy of Sciences, 730000 Lanzhou, China

[2] University of Chinese Academy of Sciences, 10049 Beijing, China

[3] Institute of Atmospheric and Earth Sciences, University of Helsinki

[4] Research Computing Center, Lomonosov Moscow State University, Moscow, Russia

[5] Moscow Center for Fundamental and Applied Mathematics, Moscow, Russia

[6] Department of Ecohydrology, Leibniz-Institute of Freshwater Ecology and Inland Fisheries (IGB), Berlin, Germany

**Correspondence to: Lijuan Wen* (wlj@lzb.ac.cn)

Abstract. Ngoring Lake is the largest freshwater lake in the Qinghai-Tibet Plateau (TP). The lake water temperature was observed to be generally rising during the ice-covered period from November 2015 to April 2016. This phenomenon appeared in the whole water column, with slowing in deep water and accelerating in shallow water before ice melting. The process is different from low-altitude boreal lakes. There are few studies on its mechanism and effects on lake-atmosphere interaction. Based on the observation data of Ngoring Lake Station, ERA5-Land data, MODIS surface temperature data, and precipitation data of Maduo Station of China Meteorological Administration, the characteristics of water temperature rise in the ice-covered Ngoring Lake are analyzed. LAKE2.3 model, which is currently little used for TP lakes, is applied to explore the influence of local climate characteristics and the main physical parameters on the radiation transfer in water body. The study questions are the continuous rise of water temperature in the ice-covered period, and the effects of different water temperature profiles prior to ice breakup on the lake heat storage per unit area and sensible and latent heat release. The results show that LAKE2.3 represents well the temperature evolution and thermal stratification in Ngoring Lake, especially in the ice-covered period. The strong downward short-wave radiation plays a dominant role, low precipitation gives

https://doi.org/10.5194/tc-2021-398
Preprint. Discussion started: 14 February 2022

positive feedback, and smaller downward long-wave radiation, lower temperature and larger wind speed give negative feedback. Increase of ice albedo and ice extinction coefficient reduces the heating rate of water temperature before reaching the maximum density temperature, and increases the maximum temperature that can be reached during ice-covered period, while increasing the water extinction coefficient has little influence on water temperature. The lake temperature in Ngoring Lake rising during the ice-covered period, and the temperature at the upper layer of lake body was higher than that at the maximum density temperature before ice breaking. Compared with the characteristics of three typical ice-covered periods which the lake temperature remained fixed in each layer, and the lake temperature was less than or equal to the maximum density temperature, the difference of heat release after ice breaking lasted for 59-97 days. The higher the lake temperature before breakup, the more heat is stored in the lake, and the more sensible heat and latent heat is released when the ice melts completely and the faster is the heat release.

1 Introduction

The Tibetan Plateau (TP), with an average altitude of 4000-5000 m, is known as the "roof of the world". It is the highest plateau on Earth. There are many alpine lakes in TP constituting the largest number, largest area and highest altitude plateau lake group in China, known as the "Asian water tower" (Immerzeel et al., 2010). There are more than 1400 lakes with an area of more than 1 km^2, and the total area of lakes is more than 5×10^4 km^2, accounting for 57.2 % of the total lake area in China (Wan et al., 2016; Zhang et al., 2019).

Lakes are sensitive to climate change and therefore act as indicators of climate change (Adrian et al., 2009; Qin et al., 2009). Under the background of global warming, the surface temperature of lakes has been rising (O'Reilly et al., 2015; Schmid et al., 2014; Sharma et al., 2015; Zhang et al., 2014). The warming rate of the TP is twice the global average. Among the 52 plateau lakes surveyed, the surface temperature of 60 % of the lakes shows an upward trend, while the surface temperature of some lakes shows a downward trend due to the melting of glaciers (Duan and Xiao, 2015; Yang et al., 2014; Zhu et al., 2020). The surface temperature affects the thermal stratification and the length of the ice-covered period, not only on the stability and vertical convection of the lake. Also the material and energy exchange between the lake and the atmosphere depend on the surface temperature (Efremova et al., 2013; Ramp et al., 2015; Rösner et al., 2012) that has impact on the local climate (Gerken et al., 2013; Li et al., 2016a; Wen et al., 2015; Xu and Liu, 2015; Yang and Wen, 2012).

At the same time, lake temperature is an important indicator of lake ecosystem

https://doi.org/10.5194/tc-2021-398
Preprint. Discussion started: 14 February 2022

restricting the biochemical process inside the lake. The temperature not only changes the content of dissolved oxygen, nitrogen, phosphorus and other nutrients but also changes the rate of biochemical reactions, thus affecting the water quality and distribution of aquatic organisms in the lake (Dokulil, 2013; Hardenbicker et al., 2016; Li et al., 2015a; Weitere et al., 2010). Lake ecology is an important part of the Tibetan Plateau ecosystem. Therefore, it is of great significance to study the characteristics of lake temperature for understanding the plateau aquatic ecosystem in the local weather and climate conditions.

Due to the variations of latitude, altitude and depth, the lake temperature characteristics are different in lakes of different geographical regions. Tropical and subtropical lakes possess high temperature throughout the year, and in winter, they do not freeze and are not affected by ice. For example, Kivu Lake, a tropical lake located in central Africa, has a winter temperature greater than 20 °C (Thiery et al., 2014), and Taihu, a subtropical lake located in the middle and lower reaches of the Yangtze River in China, and Mangueira Lake, a subtropical lake located in Rio Grande do Sul, have a winter temperature greater than 5 °C (Tavares et al., 2019; Chen et al., 2021). However, the boreal lakes located in middle and high latitudes usually freeze in winter, and the increase of the lake surface albedo due to ice cover affects the radiation transfer into water body and, consequently, the lake temperature (Erm et al., 2010). Among lakes located in middle and high latitudes but at a low altitude, the under-ice water of some lakes is evenly mixed in winter, and the temperature of the entire lake is basically maintained at a temperature between 0-$T_{\rho,max}$ ($T_{\rho,max}$ is the maximum density, $T_{\rho,max}$ = 3.98 °C for fresh water). Such lakes are, for example, Sunapee Lake, a northern temperate lake in New Hampshire, Simcoe Lake in southern Ontario, Canada, and Mendota Lake in the United States (Bruesewitz et al., 2015; Yang et al., 2017; Yang et al., 2021). Another class of mid- and high-latitude lakes have an inverse winter stratification. The ice-water interface temperature is at the freezing point, and the deeper water temperature is the highest, at most $T_{\rho,max}$, and the temperature in each layer is maintained at a temperature between the freezing point and $T_{\rho,max}$. Temperature increases from the upper layer to the lower layer in such lakes as Thrush Lake in Northestren Minnesota (Fang and Stefan, 1996), Pääjärvi Lake located in southern Finland (Saloranta et al., 2009) and Valkea-Kotinen Lake (Li et al., 2016b). Their vertical temperature profiles are different, but the temperature is between the freezing point and $T_{\rho,max}$ during ice-covered period. Therefore, we present the question: what are the winter temperature characteristics of high-altitude lakes?

Due to the harsh environment of the TP and difficulties in collecting field observations, field studies have been limited to several large lakes such as Nam Co, Bangong Co, Qinghai Lake, Ngoring Lake, and most of them have been performed in ice-free period

https://doi.org/10.5194/tc-2021-398
Preprint. Discussion started: 14 February 2022

(Lazhu et al., 2015; Su et al., 2020; Huang et al., 2019; Song et al., 2020). It has been found out that in several lakes in TP the temperature rises during the ice-covered period. The temperature of Bangong Co and Nam Co Lakes have risen from freezing to melting, but the rise is greater in the latter due to the difference in lake depth. The temperature in Dagze Co Lake remained fixed in each layer in the early ice-covered period and began to rise in the late ice-covered period, because this lake is meromictic with high salt content (Wang et al., 2014; Lazhu et al., 2021; Wang et al., 2021). Ngoring Lake is the largest and relatively shallow freshwater lake on the TP. Its temperature has been rising throughout the whole ice-covered period, and studies show that solar radiation transfer plays an important role in this process (Wang et al., 2021; Kirillin et al., 2021). Although previous studies have revealed the warming phenomenon of TP lakes during ice-covered period with qualitative analysis pointing out that temperature rise is affected by salinity and depth (Lazhu et al., 2021), they did not consider the influence of ice, meteorological conditions, and physical processes in the warming.
Numerical models are often used to reveal the phenomena and mechanisms of TP lakes. At present, the lake models widely used in the TP are the Flake model (Freshwater Lake Model) and the lake scheme coupled in the CLM model (Community Land Model) CoLM (Common Land Model), and WRF (Weather Research and Forecasting Model) (Fang et al., 2017; Lazhu et al., 2016; Wen et al., 2016; Song et al., 2020; Dai et al., 2018; Huang et al., 2019; Wu et al., 2021). However, the simulated water temperatures in winter by the two models kept stationary and could not reproduce the observed rising temperature (Lazhu et al., 2016; Wen et al., 2016; Huang et al., 2019).
This paper 1) applies the LAKE model for a typical TP lake to evaluate its capability to simulate the rising lake temperature in ice-cover period; 2) uses the LAKE model to analyze the influence of the meteorological driving factors and the main parameters that affect the radiation transmission on the warming process during the ice season in Ngoring Lake; 3) discusses the influence of temperature distribution prior to ice breakup on lake heat storage and lake-air heat transfer.

2 Study Area and Data

2.1 Study Area

Ngoring Lake (34.76º N-35.08º N, 97.53º E-97.90º E, Fig. 1) is located in the western valley of Maduo County on the eastern TP, with an average lake surface elevation of 4274 m a.s.l. It is the largest freshwater lake in the Yellow River source region. Its surface covers an area of 610 km^2, and the maximum and average depth are 32 and 17 m, respectively. The pH is 8.49 and there are only few fish in the lake. Aquatic plants

https://doi.org/10.5194/tc-2021-398
Preprint. Discussion started: 14 February 2022

grow only in the riparian area. The lake is thermally stratified in summer and ice-covered from the end of November or early December to late April (Wen et al., 2016). Ngoring Lake basin is dominated by the cold, semi-arid continental climate, which is sensitive to the Westerly jet, Indian monsoon and Asian monsoon (Zhang et al., 2013). According to observation data from 1953 to 2016 at Maduo Station (34.9º N, 98.2º E) of China Meteorological Administration, the average annual precipitation was 322.4 mm, mostly concentrated in May to September. The average annual air temperature was -3.53 ºC, and the maximum and minimum air temperature were 24.3 ºC and -48.1 ºC, occurred in July 20, 2006 and January 2, 1978, respectively.

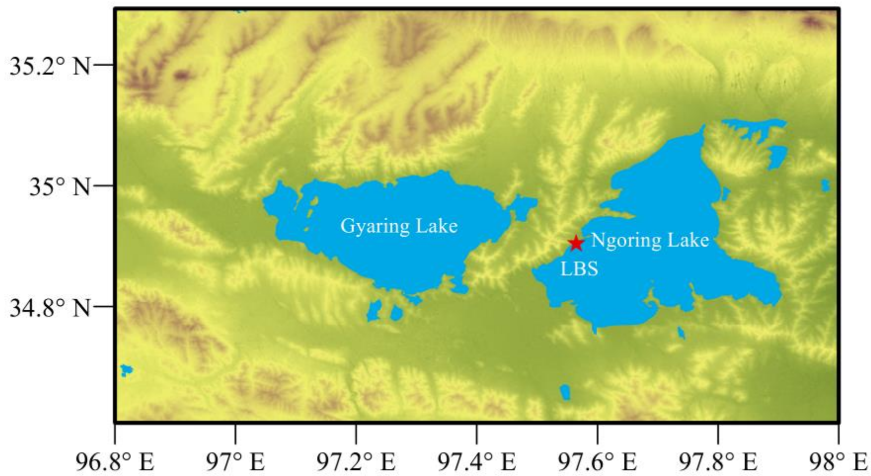

Figure 1. Location of Ngoring Lake, and the pentagram denotes the lake border station (LBS).

2.2 Data

2.2.1 LBS Station Data

The long-term autonomous lake border station (LBS) has an altitude of 4282 m above sea level, installed at 34.91º N and 97.55º E in October 2012 (Fig. 1). It provided 10 m altitude wind speed, 2 m altitude air temperature, specific humidity and air pressure, and 1.5 m altitude downward shortwave (SR) and longwave radiation (LR) from September 22, 2015 to September 22, 2016 as the driving data for the model (Li et al., 2020). Li et al. (2015b) and Wen et al. (2016) are referred for the detailed information about the site configuration and measured quantities. Precipitation intensity was calculated according to the accumulated precipitation of Maduo Station from 20:00 to 20:00 the next day in the daily value data set (V3.0) of Chinese surface climate data (http://data.cma.cn). The water temperature profile was observed in the northern part of Ngoring Lake, where the water depth was 23-25 m in 2015-2016 (Li et al., 2020).

2.2.2 MODIS Lake surface temperature

The Land Surface Temperature 8-Day L3 Global product (MYD11C2), which is derived from the data of Moderate Resolution Imaging Spectroradiometer (MODIS), was used to determine the ice-covered period in the Ngoring Lake and to verify the simulated results, due to the lack of ice thickness and water surface temperature observations. MODIS provides daily global coverage with high spatial resolution on a long-term basis. The product which is obtained by synthesizing and averaging values from the corresponding eight MYD11C2 daily files provides the land surface temperature (LST) at a resolution of 0.05º latitude/longitude (5600 m at the equator) for Climate Modeling Grid (CMG) (https://ladsweb.nascom.nasa.gov/search) (Wan et al., 2004).

2.2.3 ERA5-Land Data

ERA5-Land is produced as an enhanced global dataset for the land component of the fifth generation of European ReAnalysis (ERA5) by the European Centre for Medium-Range Weather Forecasts (ECMWF), framed within the Copernicus Climate Change Service (C3S) of the European Commission. It is available for hourly ERA5-Land record for 40 years from 1981 to the present, and ERA5-Land back extension (1950-1980) is in preparation. Compared to ERA5 (31 km) and ERA-Interim (80 km), ERA5-Land has enhanced horizontal resolution of 9 km (~0.08º). It is convenient for users to interpolate data into the longitude and latitude grid of 0.1º spacing (https://cds.climate.copernicus.eu/cdsapp#!/dataset/reanalysis-era5-land?tab=form) (Hersbach et al., 2020; Muñoz-Sabater et al., 2021).

3 Methods

3.1 LAKE Model

The one-dimensional lake model LAKE, including thermodynamic, hydrodynamic and biogeochemical processes, is used to solve the horizontally averaged transfer equations of gases, heat, salinity and momentum in an enclosed water body (Stepanenko et al., 2016; Stepanenko et al., 2011). The vertical heat transfer is simulated, and the penetration of SR in water layers (Heiskanen et al., 2015), ice, snow and bottom

https://doi.org/10.5194/tc-2021-398
Preprint. Discussion started: 14 February 2022

sediments (Cao et al., 2020) is taken into account. The exchange between water and inclined bottom is modelled explicitly because the model equations have been averaged over horizontal sections of a water body. The κ-ε parametrization of turbulence is applied (Stepanenko et al., 2016).

3.1.1 Heat transfer in water body

The water temperature is calculated according to the one-dimensional thermal diffusion equation:

$$c_w\rho_w\frac{\partial T_w}{\partial t}=-c_w\rho_w\frac{1}{A}\int_{\Gamma_A}T_w\,(u_h\cdot n)dl+\frac{1}{Ah^2}\frac{\partial}{\partial\xi}\left(AK_T\frac{\partial T_w}{\partial\xi}\right)-\frac{1}{Ah}\frac{\partial AS}{\partial\xi}+$$

$$c_w\rho_w\frac{dh}{dt}\frac{\xi}{h}\frac{\partial T_w}{\partial\xi}+\frac{1}{Ah}\frac{\partial A}{\partial\xi}\left[S_b(\xi)+F_{iz,b}(\xi)\right]\ ,\qquad (1)$$

where c_w is heat capacity of water, ρ_w is density of water, T_w is temperature of water, $h(t)$ is lake depth, t is time, $\xi=z/h$ is a normalized vertical coordinate, $z=0$ ($z\in[0,h]$) is located at the free surface of the lake, S is downwelling shortwave radiation, A is the z-dependent cross-sectional area of water, K_T is thermal diffusivity coefficient equal to the sum of molecular and turbulent diffusivities, $S_b(\xi)$ is shortwave radiation flux, $F_{iz,b}$ is soil heat flux at the level z, n is an outer normal vector to the boundary Γ_A of the horizontal cross section A and u_h is horizontal vector in water (Stepanenko et al., 2016; Guseva et al., 2016). The solar radiation penetrated into the water is calculated using the Beer-Lambert law (Stepanenko and Lykossov, 2005; Stepanenko et al., 2019):

$$S(\xi)=S(0)\exp(-a_e h\xi)\ ,\qquad (2)$$

where a_e is extinction coefficient. In order to solve the temperature in Eq. (1), it is necessary to specify the top and bottom boundary conditions and to give the method to calculate the edge heat flux at each depth z. The atmospheric turbulent heat flux schemes are based on the Monin-Obukhov similarity theory, and the top boundary condition is a perfect heat balance equation (Stepanenko et al., 2016). When the lake is covered with ice, the temperature of the last layer of ice and the first layer of layer of water are equal and fixed to the melting point temperature (Stepanenko et al., 2019), which is calculated by the following formula:

$$T_{mp}=-C*\left|\partial T_{mp}/\partial C\right|\ ,\qquad (3)$$

where T_{mp} is the melting point temperature (°C), C is salinity at the water-ice interface, $\left|\partial T_{mp}/\partial C\right|$ = 66.7 °C is assumed constant.

https://doi.org/10.5194/tc-2021-398
Preprint. Discussion started: 14 February 2022

3.1.2 Heat transfer in snow cover

Snow cover is formed by accumulation of precipitation during the cold season. It is characterized by liquid water content and temperature. The equations are as follows:

$$c_{sn}\rho_{sn}\frac{\partial T_{sn}}{\partial t} = \frac{\partial}{\partial z}\lambda_{sn}\frac{\partial T_{sn}}{\partial z} + \rho_{sn}LF_{fr} - \frac{\partial S}{\partial z}\ , \qquad (4)$$

$$\frac{\partial W}{\partial t} = -\frac{\partial \gamma}{\partial z} - F_{fr}\ , \qquad (5)$$

where c_{sn} is specific heat of snow, ρ_{sn} is density of snow, T_{sn} is temperature of snow, λ_{sn} is thermal diffusivity of snow, L is latent heat of melting, F_{fr} is rate of freezing, W is liquid water content and γ is filtration flux of liquid water (Stepanenko and Lykossov, 2005).

3.1.3 Heat transfer in ice cover

The heat conduction equation in ice cover follows the equation:

$$c_i\rho_i\frac{\partial T_i}{\partial t} = c_i\rho_i\frac{\xi}{h_i}\frac{dh_i}{dt}\frac{\partial T_i}{\partial \xi} - c_i\rho_i\frac{1}{h_i}\frac{dh_{i0}}{dt}\frac{\partial T_i}{\partial \xi} - \frac{1}{h_i}\frac{\partial S}{\partial \xi} + \frac{1}{A_i {h_i}^2}\frac{\partial}{\partial \xi}\left(A_i\lambda_i\frac{\partial T_i}{\partial \xi}\right) + \frac{1}{A_i h_i}\frac{\partial A_i}{\partial \xi}F_{T,b} - L\rho_i\frac{dp}{dt}\ , \qquad (6)$$

where c_i is specific heat of ice, ρ_i density of ice, T_i is temperature of ice, λ_i is thermal conductivity of ice, h_i is ice thickness, $\frac{dh_{i0}}{dt}$ is the increment of ice thickness on its surface, $F_{T,b}$ is the heat flux at the ice-sediment boundary, A_i is the z-dependent cross-sectional area of the ice cover determined by the basin morphometry, L is the freezing/thawing heat of water and p is ice porosity (Stepanenko et al., 2019).

Based on the study of Leppäranta (2014), the albedo regulates the surface energy budget, and the extinction coefficient controls the vertical distribution of radiation energy in the medium. In the LAKE model, the albedo of water (A_w) is 0.06, and the extinction coefficient of snow (E_s) decreases with the increase of snow density. Snow accumulation in the Ngoring Lake area is basically zero, and therefore, only the A_i, the E_i and E_w are analyzed in this study. The model used in this article is version 2.3 of the LAKE model, called LAKE2.3.

This model has been widely used. Thiery et al. (2014) compared and evaluated seven models in LakeMIP by using Kivu Lake, one of the five Great Lakes in Africa. It was found that the LAKE model can better simulate the vertical mixing process and internal thermal stratification of Kivu Lake than Flake and Hostetler models. Stepanenko et al. (2016) found that the LAKE model can reproduce the temperature of Kuivajärvi Lake and the vertical distribution of dissolved gases in summer.

3.2 Validation Methods

The indexes to evaluate the accuracy of the model are the root mean square error ($RMSE$), *BIAS,* and correlation coefficient (CC):

$$RMSE = \sqrt{\frac{1}{n}\sum_{i=0}^{n}(m_i - o_i)^2} \quad , \qquad (7)$$

$$BIAS = \bar{m} - \bar{o} \quad , \qquad (8)$$

$$CC = \frac{\mathrm{Cov}(M,O)}{\sqrt{\mathrm{Var}(M)\,\mathrm{Var}(O)}} \quad , \qquad (9)$$

where m_i represents the simulations and o_i represents the observations, $\bar{m}$ is the average value of simulations and $\bar{o}$ is the average value of observations. $\mathrm{Cov}(M,O)$ is the covariance of observed and simulated values. $\mathrm{Var}(M)$ and $\mathrm{Var}(O)$ are the variances of simulated and observed values, respectively.

3.3 Calculation Method of Heat Storage

The evolution of the heat storage per unit area in the water is calculated by using the changes of water temperature profiles

$$\Delta Q = c\rho \sum_{i=1}^{n} T_i \Delta z_i \quad , \qquad (10)$$

where c = 4192 J kg^{-1} K^{-1} and ρ = 10^3 kg m^{-3}, n is the number of depths, Δz_i is the depth interval between two layers and ΔT_i is the temperature change in layer *i* (Gan and Liu, 2020; Nordbo et al., 2011).

4 Characteristics Analysis

4.1 Characteristics of Observed Water Temperature

4.1.1 Ngoring Lake

According to the observations in Ngoring Lake, the water temperature has increased continuously during the winter ice-covered period (Wang et al., 2021; Kirillin et al., 2021). From the observed water temperature profile (Fig. 2a), it can be seen that the temperature reached its lowest point in early December 2015, then the lake froze over, and the water under ice warmed and was completely mixed in the early stage of the ice season. From mid-March onward, the water body showed weak stratification with temperature decreasing downward with 5.2 °C at 2 m dept and 3.9 °C at the bottom**.** By mid-April, the ice melted completely, and after that full mixing took place.

https://doi.org/10.5194/tc-2021-398
Preprint. Discussion started: 14 February 2022

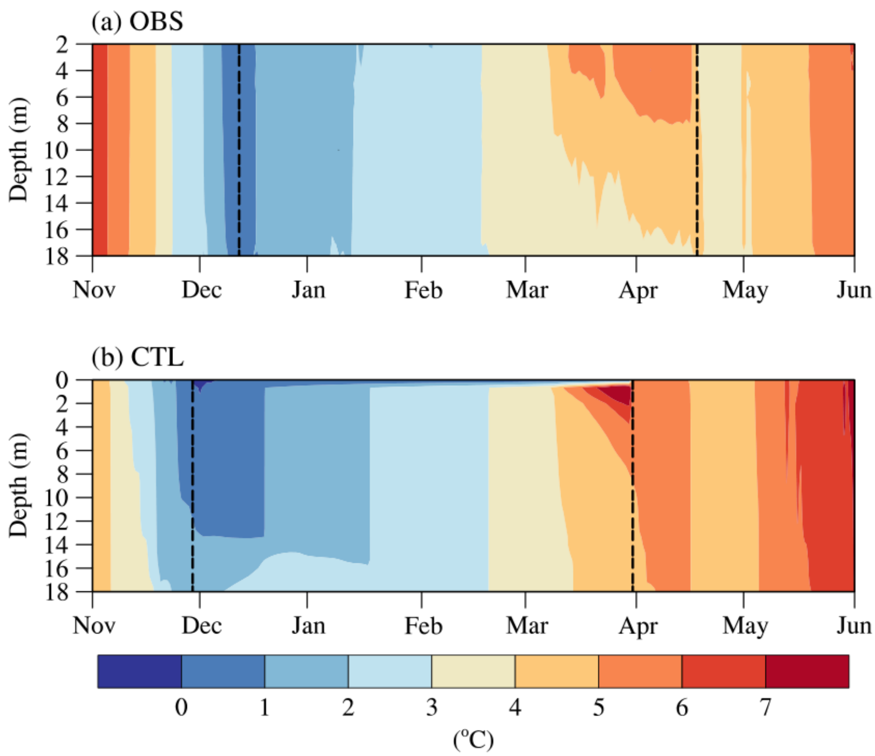

Figure 2. The daily average water temperature (a) observed and (b) simulated in CTL from November 2015 to June 2016. Ice-covered period is represented between the two black dotted lines.

In order to more intuitively analyze the changes of lake temperature over time, the observed water temperature of Ngoring Lake was averaged daily (Fig. 3a). The lake was mixed completely in early November 2015, and the water temperature decreased gradually. In late November, the temperature oscillated and the difference between 2 m and 22 m was less than 1 °C. On December 12, the water temperature reached the lowest point, at 2 m it was 0.47 °C. At this time, the lake was completely frozen, and the air temperature at 2 m height was -7.79 °C. Thereafter, the lake was mixed, and then the temperature showed new oscillations from early January for about one month (Kirillin et al., 2021). In mid-February, the lake was again fully mixed, and the water temperature continued to rise, reaching $T_{\rho,max}$ on March 7. Thereafter, as the water continued to absorb the strengthening solar radiation, the lake began to stratify, since absorption of radiation decays with depth according to the Beer-Lambert law. The water temperature continued to rise in the upper layer (2-6 m) by the rate ~0.052 °C d^{-1}, which was higher

https://doi.org/10.5194/tc-2021-398
Preprint. Discussion started: 14 February 2022

The Cryosphere Discussions
Open Access
EGU

than before March 7 (~0.035 °C d^{-1}). On April 18, the ice had melted completely, and the water temperature rose to a maximum of 5.83 °C at 2 m while remaining at $T_{\rho,max}$ below 10 m depth. Having reached the open surface state, full mixing took place rapidly, and then the lake warmed gaining heat from the atmosphere.

4.1.2 Kilpisjärvi Lake

Different from Ngoring Lake, the temperature of some lakes can remain fairly stable in each layer during ice-covered period, such as Thrush Lake, Valkea-Kotinen Lake, Pääjärvi Lake and Kilpisjärvi Lake (Fang and Stefan, 1996; Saloranta et al., 2009; Li et al., 2016b; Tolonen, 1998). Among these lakes, we paid special attention to Kilpisjärvi Lake.

Kilpisjärvi Lake (K Lake, 69.05º N, 20.83º E, 473 m a.s.l.) is an Arctic tundra lake located in northern Finland. The latitude difference is about 34°, the longitude difference is about 77° and the altitude difference is about 3800 m between Ngoring Lake and K Lake. The temperature decreases with altitude at a rate of 6 °C km^{-1} (Jiang et al., 2016), and according to present general climatology, in Eastern Europe/Central Asia the latitudinal and longitudinal decreases in winter are about 1.2 °C deg^{-1} and 0.3 °C deg^{-1}, respectively. Therefore, an increase of 1 km in altitude is equivalent to an increase of 5° in latitude or 20° in longitude. Between Ngoring and K Lake, the effects of altitude, latitude and longitude on air temperature offset each other, and there was only little difference in air temperature between the two sites (Fig. 4f). However, apart from the surface layer, the water temperature of K Lake basically maintained at $T_{\rho,max}$ during the ice-covered period (Fig. 3b). Therefore, we suspected that the warming characteristics of Ngoring Lake were related to the local climate, and to show that we shall analyze the climate characteristics of the two sites in Sect. 4.2.

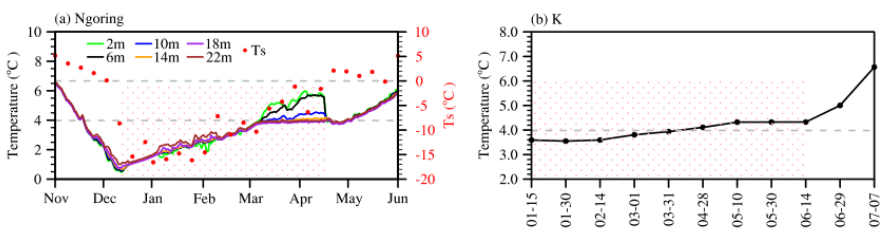

Figure 3. (a) The daily average water temperature observations of Ngoring Lake at the surface (Ts), 2 m, 6 m, 10 m, 14 m, 18 m and 22 m from November 2015 to June 2016, and (b) the average water temperature observations of K Lake from 5 m to 30 m in 1993. Ts is MODIS surface water temperature. The gray reference lines denote $T_{\rho,max}$ = 3.98 °C and 0 °C, respectively. The pink shaded areas denote

https://doi.org/10.5194/tc-2021-398
Preprint. Discussion started: 14 February 2022

ice-covered period.

4.2 Characteristics of Local Climate

The daily averages of meteorological variables near the two lakes are shown in Fig. 4 during November to June, and the ranges and averages from December 12 to April 18 of the next year (ice-covered period of Ngoring Lake) were compared (Table 1). The differences in the average air temperature, specific humidity and downward LR between Ngoring Lake and K Lake were -0.42 °C, -0.38 g kg^{-1} and 41.9 W m^{-2}, respectively. The wind speed of Ngoring Lake was 1.7 times that of K Lake, and the downward SR was 159.0 W m^{-2} greater in Ngoring Lake than in K Lake. However, the precipitation was much less in Ngoring Lake than in K Lake, by the factor of 0.037. In general, there were not many differences in temperature, specific humidity and downward LR between the two places, but there was lower precipitation, and higher downward SR and wind speed in the TP. Since the surface pressure has little effect on water temperature, this paper does not consider that.

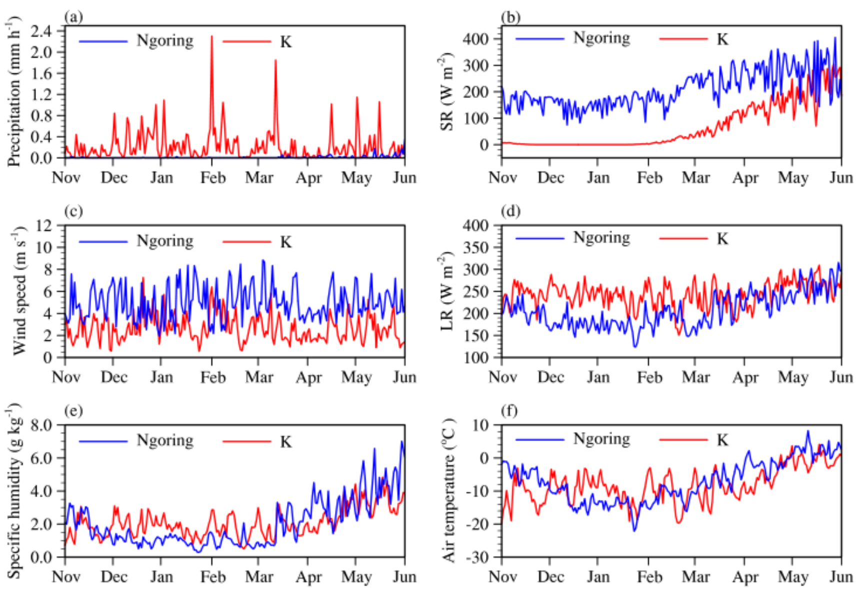

Figure 4. Comparison of daily average values of the climate field for Ngoring Lake from November 2015 to June 2016 and for K Lake with the same month from 1992 to 1993. (a) precipitation, (b) downward SR, (c) wind speed at 10 m height, (d) downward LR, (e) specific humidity and (f) air temperature at 2 m height. The driving field of K Lake was extracted from ERA5-Land data.

https://doi.org/10.5194/tc-2021-398
Preprint. Discussion started: 14 February 2022

Table 1. The range and mean values of the driving meteorological variables of Ngoring Lake (2015-2016) compared with K Lake (1992-1993) during the ice-covered period (12.12-4.18).

Meteorologic variables	Ngoring Lake		K Lake	
	Range	Average	Range	Average
Precipitation (mm h^{-1})	< 0.072	0.0044	< 1.15	0.12
Downward SR (W m^{-2})	73.98-356.29	199.41	< 186.84	40.46
Wind speed (m s^{-1})	1.95-8.85	4.93	0.56-7.28	2.83
Downward LR (W m^{-2})	123.92-271.60	191.73	150.61-289.59	233.62
Specific humidity (g kg^{-1})	0.29-4.52	1.40	0.50-3.23	1.78
Air temperature (°C)	-22.16-2.24	-10.25	-19.69--2.01	-9.83

5 Simulation Setup

In order to reveal the mechanism of water temperature increase during ice-covered period in Ngoring Lake and its influences, we set up one control simulation (CTL) and 28 experimental simulations (SIM) in this study (Table 2).

5.1 Setup in CTL

The depth of Ngoring Lake was set as 26.5 m, which is the depth at the water temperature site, and the vertical stratification was described by 35 layers. The simulation period was from September 2015 to September 2016. The initial vertical profile of water temperature, and the mixed layer and the bottom temperature were set according to the observations (Fig. 2a). The albedo of snow and ice and the extinction

https://doi.org/10.5194/tc-2021-398
Preprint. Discussion started: 14 February 2022

coefficients of ice and water were set as, respectively, $A_s = 0.7$, $A_i = 0.25$, $E_i = 2.5\ m^{-1}$ and $E_w = 0.15\ m^{-1}$ on the basis of previous investigations (Lei et al., 2011; Li et al., 2018; Li et al., 2020; Shang et al., 2018). The driving meteorological input variables were air pressure, wind speed, specific humidity, air temperature, precipitation, downward SR and LR. The driving data time step was 30 minutes, and the model time step was 15 seconds.

5.2 Setup in SIM

In order to explore the influences of climate field, the simulation called SIM_KinN was set up where all the forcing variables were replaced by those of K Lake on the basis of CTL. In order to explore the influence of a single meteorological variable, SIM_* simulations (* is SR, Precip, LR, U, Tair or q) were set up, where the * variable was replaced by the K Lake variable on the basis of CTL. These scenarios were quite artificial because climate variables are actually closely correlated. Nevertheless, using the sensitivity simulations can shed light on the influence of climate on lake temperature evolution during ice-covered period.

In order to explore the influence of main physical parameters, SIM_# (# is the value of A_i, E_i or E_w) is set up, representing the simulation when A_i, E_i or E_w was equal to # on the basis of CTL, respectively.

SIM_E* (* represents 1, 2 or 3) is set for exploring the effects of different water temperature profiles before ice-melting on the lake heat storage and heat fluxes, which represents three different vertical lake water temperature profiles on March 25, 5 days before the ice breaking.

Table 2. Names, explanations and corresponding numbers of all experiments.

Experiment name	Experiment introduction	Number
CTL	Control simulation	1
SIM_KinN	The simulation when all the drive variables are replaced by those of K Lake on the basis of CTL.	1
SIM_* (* represents meteorological variables)	The simulation when the * variable is replaced by that of K Lake on the basis of CTL.	6
SIM_#	The simulation when the physical variable is	18

https://doi.org/10.5194/tc-2021-398
Preprint. Discussion started: 14 February 2022

(# represents values of A_i, E_i or E_w)	equal to # on the basis of CTL, respectively.	
SIM_E* (* represents 1, 2, and 3)	The simulation when using three different initial temperature profiles on the basis of CTL.	3

6 Simulation Results

6.1 Model Validation

Compared with the observations (Fig. 2a), the simulation results of CTL (Fig. 2b) were basically consistent with the observations, but the whole ice season was shifted to occur about half a month earlier than observed. The water temperature was slightly higher from mid-March to the end of May in the model compared with observations, and there were differences in the simulation of deep layers. After the ice had melted, the simulated temperature rose faster and was about 1 ℃ higher than the observed value. In general, LAKE2.3 can reproduce the thermal stratification at the end of ice season in Ngoring Lake.

The simulation was evaluated by comparing *RMSE, BIAS, CC* (Table 3) of the simulated and observed water temperature at lake surface, 2 m, 9 m, 14 m and 22 m in Ngoring Lake from November 2015 to June 2016 (Fig. 5a-e). It can be seen that *CC* of each layer was greater than or equal to 0.95, and the *CC* of 2 m, 9 m and 14 m were as high as 0.98, but *RMSE* and *BIAS* of lake surface were larger, 3.25 ℃ and 1.42 ℃, respectively. The surface temperature error was largely owing to the inaccuracy of the MODIS data (Donlon et al., 2002; Tavares et al., 2019). The absolute value of *BIAS* of other layers was less than 0.01 ℃, and *RMSE* was less than 0.95 ℃. In addition, it can be concluded that the simulation of the temperature rise in the ice-covered period was good, and the maximum temperature was 0-1 ℃ higher than the observed value.

In conclusion, LAKE model can simulate the lake warming phenomenon under ice cover good in Ngoring Lake, because in the presence of ice and snow cover, the water temperature of the first layer (0 m) is determined by the freezing point (Eq. 3) and does not depend on air–lake heat exchange, and the solar energy is transferred from the first layer to ice bottom or to the second layer. With the increase of depth, the solar energy absorption decays. Thus, the second layer gains the most of solar heating, while the deeper water temperature maintains at $T_{\rho,max}$. The upper layer is less dense, the stratification is stable, and convection does not occur.

https://doi.org/10.5194/tc-2021-398
Preprint. Discussion started: 14 February 2022

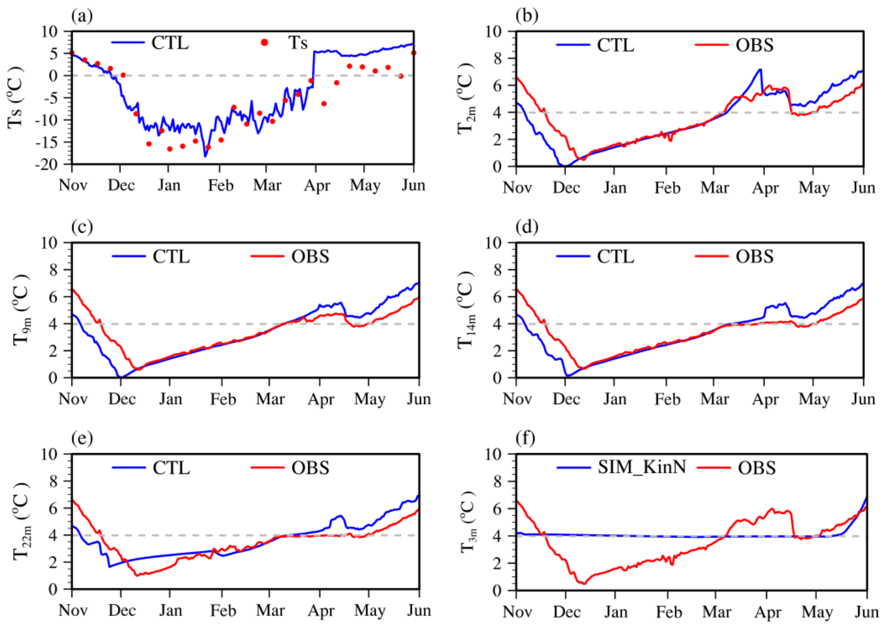

Figure 5. The daily average water temperature observed and simulated in CTL of (a) the surface (Ts), (b) 2 m, (c) 9 m, (d) 14 m and (e) 22 m in Ngoring Lake from November 2015 to June 2016. (f) Comparison of simulated in SIM_NinK and observed 3 m water temperature in Ngoring Lake. The dotted line represents $T_{p,max}$ = 3.98 °C.

Table 3. *BIAS*, *RMSE* and *CC* between simulation and observation corresponded to Fig. 5.

	Ts	T_{2m}	T_{9m}	T_{14m}	T_{22m}
BIAS (ºC)	1.42	0.04	0.09	-0.05	0.06
RMSE (ºC)	3.25	0.92	0.89	0.87	0.89
CC	0.96	0.98	0.98	0.98	0.95

6.2 Influences of Local Climate on Water Temperature

In order to explore the influences of local climate characteristics on the warming, water temperature and stratification of lakes, we designed 7 simulations, namely, SIM_* (* represents 6 meteorological variables) and SIM_KinN (Table 1). Since the water

https://doi.org/10.5194/tc-2021-398
Preprint. Discussion started: 14 February 2022

temperature at different depths changed consistently with time, the water temperature at 3 m was selected to analyze the simulation results.

SIM_SR was the simulation of Ngoring Lake when the downward SR of K Lake was substituted for the forcing. During the ice-covered period, the downward SR of CTL was strong, with an average of 199.41 W m^{-2}, while SIM_SR was 40.46 W m^{-2}, with a difference of 158.95 W m^{-2} with CTL. In the sensitivity experiment SIM_SR, the water temperature of 3 m was stable keeping in the range of 0-0.1 °C (Fig. 6a). The date of ice formation was earlier and the melting date was delayed, which led to the growth of the whole ice-covered period. Compared with CTL, the depth of the mixed layer increased (Fig. 6d). Thus, during the ice period, the strong downward SR on the TP caused the water temperature to rise, because SR in Ngoring Lake transferred more heat through the ice, resulting in the accumulation of heat and continuous warming of the lake.

In SIM_Precip simulation, the precipitation of K Lake was substituted for Ngoring Lake. In the sensitivity experiment SIM_Precip, the water temperature at 3 m kept horizontal in the early and then increased but did not exceed $T_{\rho,max}$ (Fig. 6a). Compared with CTL (Fig. 2b), the layering and the temperature maximum centers between March and April disappeared, and the lake was fully mixed (Fig. 6g). This was because the mean precipitation of SIM_Precip (0.12 mm h^{-1}) was approximately 30 times higher than in the CTL (0.004 mm h^{-1}) during the ice-covered period. The increase in precipitation led to more snowfall, more radiation reflected and absorbed by snow and less radiation entering water. More precipitation damped the rise in water temperature.

In SIM_LR simulation, the downward LR of K Lake was substituted for Ngoring Lake. In the ice-covered period, the average downward LR of SIM_LR was 233.62 W m^{-2}, which was larger than in CTL (191.73 W m^{-2}). In SIM_LR, the water temperature at 3 m still kept rising, and the time of complete melting of ice was earlier than in CTL, in the end of February or early March. After the ice breakup, the air temperature was lower, and the lake transferred heat to the atmosphere, and water temperature underwent a cooling process (2 °C) until reaching a new equilibrium with the atmosphere (Fig. 6b). Compared with the CTL, mixing in the ice-covered period was more uniform, the stratification between March and April was weakened, and the temperature maximum center was about 15 days earlier (Fig. 6e).

In SIM_U simulation, the wind speed of K Lake was substituted for Ngoring Lake. The wind speed of SIM_U was less than in CTL for the whole simulation period, and the average wind speed in ice-covered period was 2.21 m s^{-1}, smaller than in CTL. In the sensitivity experiment SIM_U, the water temperature at 3 m was rising, but it was about 3 °C higher than in the CTL in the whole simulation period (Fig. 6b). Due to the decrease of wind speed, the depth of mixed layer decreased, and the stability of the lake

https://doi.org/10.5194/tc-2021-398
Preprint. Discussion started: 14 February 2022

stratification increased (Fig. 6h).

In SIM_T_{air} simulation, the air temperature of K Lake was substituted for Ngoring Lake. The average air temperature difference between SIM_T_{air} (-9.83 °C) and CTL (-10.25 °C) was small, especially during the ice-covered period, about 0.42 °C. In the sensitivity experiment SIM_T_{air}, the water temperature decreased faster than in CTL, and at the end of October, the lake began to freeze no longer releasing energy to the atmosphere. The air temperature of K Lake fluctuated while the temperature of Ngoring Lake was continuously decreasing (Fig. 6f). The lake stratification was enhanced, and the maximum center of water temperature was about 10 days ahead of time (Fig. 6f).

In SIM_q simulation, the specific humidity of K Lake was substituted for Ngoring Lake. The difference of specific humidity between SIM_q and CTL were 0.38 g kg^{-1} during the ice-covered period. In the sensitivity experiment SIM_q, the simulation results were similar to the CTL, and thus the specific humidity had little effect on the water temperature (Figs. 6c and 6i).

On the whole, the stronger downward SR and lower precipitation in the TP played a positive role to increase the water temperature during the ice-covered period in Ngoring Lake. Less downward LR, lower air temperature and larger wind speed has an opposite effect, and specific humidity had no significant influence.

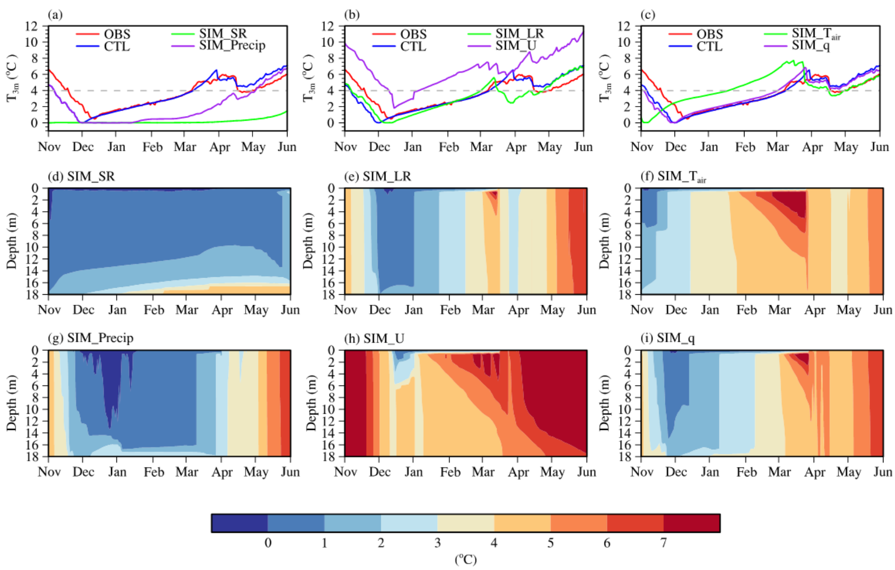

Figure 6. The simulated 3 m daily average water temperature in (a) (d) SIM_SR, (a) (g) SIM_Precip, (b) (e) SIM_LR, (b) (h) SIM_U, (c) (f) SIM_T_{air}, (c) (i) SIM_q experiments from November 2015 to June 2016 are compared with the CTL and the observation, and the change of vertical stratification is shown. The dotted line

https://doi.org/10.5194/tc-2021-398
Preprint. Discussion started: 14 February 2022

represents $T_{\rho,max}$ = 3.98 °C.

6.3 Influences of Main Physical Parameters on Water Temperature

The radiation transfer, depending on the albedo and extinction coefficient, plays a decisive role on the water temperature. The Ngoring Lake has less snow, and therefore the influence of A_i, E_i and E_w on the lake temperature simulation are discussed with sensitivity experiments. When the lake is covered by snow, the albedo of dry and light snow-covered ice is as high as about 0.9 (Leppäranta, 2014; Perovich and Polashenski, 2012). According to previous observations, Ai's observed in the TP were mostly less than 0.12, and the albedo of clear blue ice was only 0.075 (Li et al., 2018). The range of A_i without snow cover was set as 0.1-0.8 with an interval of 0.1 in the experiments SIM_A_i. E_i has not been observed on the TP, but surveys in Finnish lakes show that the value of bare ice varies between 1-4 m^{-1}, while the value of snow-covered ice can reach 5 m^{-1} (Lei et al., 2011). In SIM_E_i simulations E_i was equal to 1-5 m^{-1} with an interval of 1 m^{-1}. For the E_w, Zolfaghari et al. (2017) found that the FLake model is particularly sensitive at $E_w \leq 0.5$ m^{-1}. Shang et al. (2018) observed that E_i varies from 0.11 to 0.67 m^{-1} in a few TP lakes. Therefore, we performed the sensitivity SIM_E_w in which the E_w varied from 0.1 to 0.5 m^{-1} with an increment step of 0.1 m^{-1}. The experimental settings are shown in Table 4.

Table 4. Numerical experimental design of sensitive parameters affecting radiative transfer.

Parameter	CTL	SIM_A_i	SIM_E_i	SIM_E_w
A_i	0.25	0.1/0.2/0.3/0.4/0.5 /0.6/0.7/0.8	0.25	0.25
E_i (m^{-1})	2.5	2.5	1.0/2.0/3.0/4.0 /5.0	2.5
E_w (m^{-1})	0.15	0.15	0.15	0.1/0.2/0.3/0.4 /0.5

In the sensitivity experiment SIM_A_i, the water temperature at 3 m decreased with the increase of ice albedo, which was approximately equal to 1 °C for every step of 0.1 of the albedos. When the albedo had increased to 0.80, the rise of water temperature had decreased from 0 °C to 2 °C. The increase of ice albedo does not affect the date of ice

https://doi.org/10.5194/tc-2021-398
Preprint. Discussion started: 14 February 2022

formation, but it delayed the time of ice melting remarkably, thus prolonging the ice-covered period. When the albedo increased from 0.1 to 0.8, the increase was equivalent to 0.1-step, and the ice-covered period was extended for 15-30 days (Fig. 7a).

In the sensitivity experiment SIM_E_i, changes of extinction coefficient of ice did not all give a continuous rising of the water temperature, but at 3 m depth the temperature decreased by 1-2 °C for the increase of ice extinction coefficient by 1 m^{-1} (Fig. 7b). The greater was the extinction coefficient of ice, the more heat the ice absorbed, and the less heat entered the lake water under ice.

In order to further explore the influence of A_i on lake temperature in ice-covered period. We divided ice-covered period into two periods in CTL and the sensitivity experiment SIM_A_i and SIM_E_i, respectively Period-A and Period-B. Period-A ranged from freezing point to $T_{\rho,max}$, and Period-B ranged from $T_{\rho,max}$ to maximum temperature (T_max). The duration and heating rate of the two periods and the T_max of Period-B was calculated (Table 5 & 6). The duration of Period-A is longer than that of Period-B, and the temperature heating rate of Period-B are 10 orders of magnitude greater than that of Period-A. The reason is that lake is completely covered by ice, and the inner part of the lake is evenly mixed in Period-A, while the ice thickness decreases and the radiation absorbed by the ice decreases in Period-B. The upper layer absorbs more heat than the deeper layer, and the temperature of the upper layer increases rapidly. When A_i and E_i increases, the heating rate decreases and the duration increases in Period-A, the T_max decreases, the heating rate and duration fluctuate in Period-B. When $A_i \geq 0.6$, the heating rate during ice-covered period decreases and will not rise to $T_{\rho,max}$, so the heating rate and duration of the entire ice-covered period are shown in Table 5.

In the sensitivity experiment SIM_E_w, the water extinction coefficient had just little influence on winter water temperature, which was shown as the late ice temperature decrease with the increase of E_w (Fig. 7c). The main reason was that in the later period the ice melted and the ice thickness decreased. The higher was the extinction coefficient of water, the more heat was absorbed by shallow water and the less heat reached deep layer.

https://doi.org/10.5194/tc-2021-398
Preprint. Discussion started: 14 February 2022

The Cryosphere Discussions
Open Access
EGU

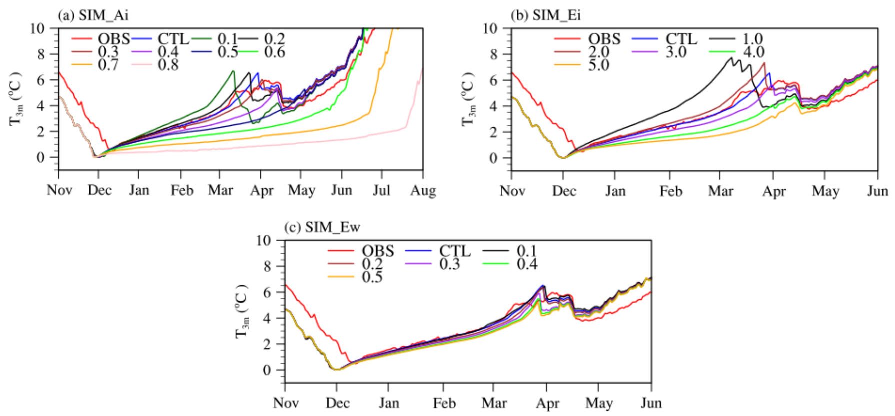

Figure 7. Comparison of the simulated daily average water temperature of 3 m with the observed value under different (a) A_i, (b) E_i, (c) E_w.

Table 5. The ice-covered period is divided into two periods which Period-A is from freezing point to $T_{\rho,max}$, Period-B is from $T_{\rho,max}$ to T_max. The duration heating rate of two periods and the T_max of Period-B is counted in SIM_A_i.

SIM_A_i	T_max (°C)	Heating Rate (°C d^{-1})		Duration (day)	
	Period-B	Period-A	Period-B	Period-A	Period-B
0.1	6.70	0.048	0.144	82	19
0.2	6.57	0.043	0.124	92	21
0.25 (CTL)	6.54	0.040	0.122	99	21
0.3	6.04	0.037	0.120	106	17
0.4	5.36	0.032	0.127	123	11
0.5	5.29	0.028	0.115	145	11
0.6	-	0.021		175	
0.7	-	0.019		207	
0.8	-	0.011		235	

*Here dashes (–) indicate no values.

https://doi.org/10.5194/tc-2021-398
Preprint. Discussion started: 14 February 2022

Table 6. The ice-covered period is divided into two periods which Period-A is from freezing point to $T_{\rho,max}$, Period-B is from $T_{\rho,max}$ to T_max. The duration heating rate of two periods and the T_max of Period-B is counted in SIM_Ei.

SIM_Ei (m^{-1})	T_max (°C)	Heating Rate (°C d^{-1})		Duration (day)	
	Period-B	Period-A	Period-B	Period-A	Period-B
1	7.53	0.059	0.101	67	35
2	7.36	0.044	0.130	91	26
2.5 (CTL)	6.54	0.040	0.122	99	21
3	5.62	0.037	0.134	109	12
4	4.73	0.033	0.052	121	14
5	4.25	0.030	0.084	132	3

6.4 Influences of Water Temperature on Lake-Atmosphere Exchange

The thermal conditions in an ice-covered lake just before ice melting have significant influence on the air-lake energy exchange. In order to explore the effects of lake temperature characteristics on the atmosphere at ice melting, three experiments – SIM_E1, SIM_E2 and SIM_E3 (Table 1) – were set up based on the CTL and the observed lake temperature profile on March 25, 2016, 5 days before the ice had completely melted (Fig. 8a). The characteristics of the initial water temperature profile were:

- SIM_E1. The stratification was weak, the temperature of the first layer was at the melting point, and, from the second layer down, the water temperature was set as 2 °C corresponding to Bangong Co (Wang et al., 2014).
- SIM_E2. The temperature was strongly stratified. The first layer was at the melting point, and the temperature increased linearly reaching $T_{\rho,max}$ at the bottom, corresponding to Valkea-Kotinen Lake (Bai et al., 2016).
- SIM_E3. The temperature of the first layer was at the melting point, and the temperature gradually increased with the depth from the second layer to the middle layer, and the temperature in the middle layer increased to $T_{\rho,max}$ corresponding to Thrush Lake (Fang and Stefan, 1996).

In the CTL, the first layer was at the melting point, and the second layer reached the maximum temperature on March 25. The deeper the layer, the lower was the temperature, until the temperature reached the higher was the temperature until reached $T_{\rho,max}$.

https://doi.org/10.5194/tc-2021-398
Preprint. Discussion started: 14 February 2022

Under the different initial temperature profiles, the heat storage per unit area of Ngoring Lake was different after ice breakup, and the difference lasted about two months (Fig. 8b). In CTL, from one day before complete melting (March 30) to complete melting (March 31), the lake heat content per unit area ranged from 30893.02 MJ m^{-2} to 30874.51 MJ m^{-2}, and the heat released was 18.51 MJ m^{-2}. In the three experiments, in the last day before ice complete melting (April 1 to 2), the heat content of the lake changed from 30657.51 MJ m^{-2} to 30651.67 MJ m^{-2} in SIM_E1, from 30781.07 MJ m^{-2} to 30769.91 MJ m^{-2} in SIM_E2, and from 30833.28 MJ m^{-2} to 30822.42 MJ m^{-2} in SIM_E3, and the heat release was 5.84 MJ m^{-2}, 11.16 MJ m^{-2}, and 10.86 MJ m^{-2}, respectively (Fig. 8b). Although the initial lake temperature profiles were different before complete melting, the higher the lake temperature was, the earlier and faster the ice melted. The heat storage per unit area of Ngoring Lake varied from March 25 to May 24, and the heat release rate of the lake was different under different circumstances. After the late May, the heat balance between the lake and the atmosphere was the same, and so the heat storage per unit area of the lake is basically the same after that.

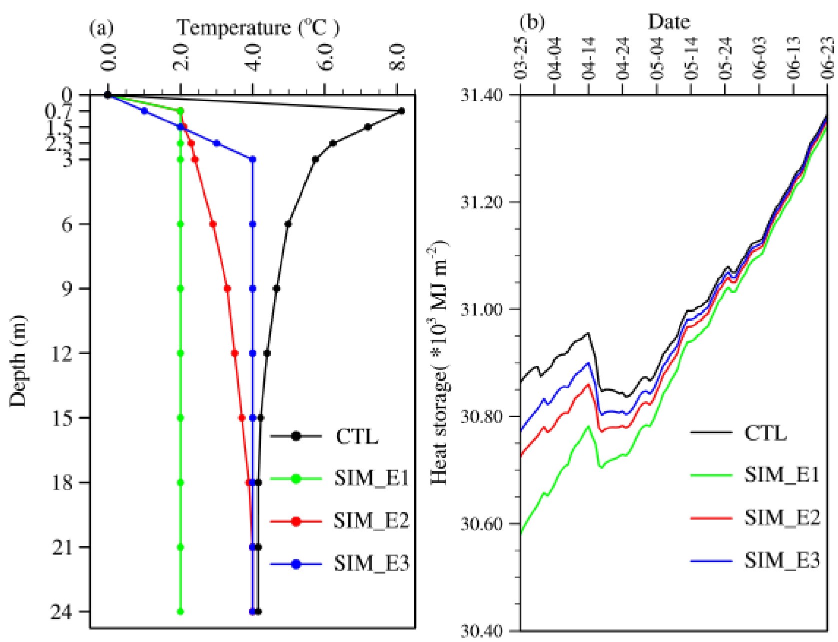

Figure 8. (a) The initial water temperature profile in the model is set on March 25, 2016 and the corresponding daily average (b) lake heat storage per unit area is simulated. SIM_E1, SIM_E2 and SIM_E3 are three different initial water temperature profiles.

https://doi.org/10.5194/tc-2021-398
Preprint. Discussion started: 14 February 2022

The temperature of the lake surface also affected the sensible and latent heat release from the lake surface. The sensible and latent heat differences between CTL and the three experimental simulations were calculated (Fig. 9). The influence of different initial water temperature profiles started in March 31, that is, when the ice had melted completely in CTL, and when the sensible and latent differences between CTL and three experimental simulations was less than 0.1 W m^{-2} for three consecutive days, we judged that the influence ended. The maximum differences of the sensible heat (51.0 W m^{-2}) and latent heat (76.7 W m^{-2}) between SIM_E1 and CTL appeared on March 31 and ended on June 12 and 30, respectively (Fig. 9a). In SIM_E2 the corresponding numbers were 51.4 W m^{-2} (March 31 to June 5) for sensible heat and 81.7 W m^{-2} (April 1 to June 17) for latent heat (Fig. 9b), and in SIM_E3 they were 51.5 W m^{-2} (March 31 to May 23) for sensible heat and 86.0 W m^{-2} (April 1 to June 5) for latent heat (Fig. 9c). Compared with the three lake temperature characteristics, the heating characteristics of Ngoring Lake made the heat release higher and faster during ice breakup. The duration of heat release difference was 59 (to May 23)-97 (to June 30) days, and for the latent heat release the situation lasted about 12-18 days longer than for the sensible heat release.

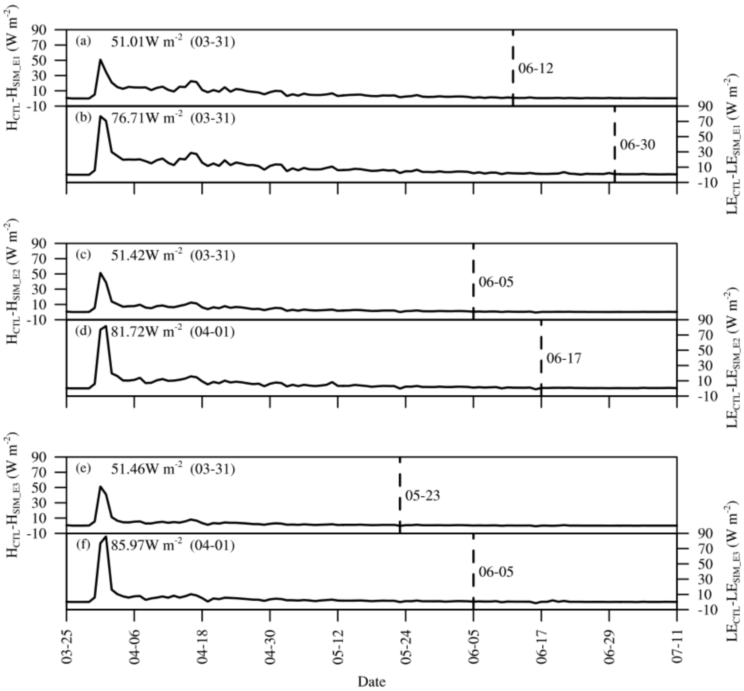

Figure 9. The daily averaged difference between the simulated sensible and latent

https://doi.org/10.5194/tc-2021-398
Preprint. Discussion started: 14 February 2022

heat and the CTL under three different initial water temperature profiles in SIM_E1, SIM_E2 and SIM_E3.

7 Conclusions

In Ngoring Lake, the largest freshwater lake on the TP, we have observed a significant increase in lake temperature during the ice-period, and this phenomenon not only occurs in Ngoring Lake but also in other TP lakes such as Bangong Co, Gongzhu Co, Zhari Namco, Dagze Co and Nam Co. The situation is largely different from the low-altitude northern lakes where the air temperature is comparable. We used the LAKE model combined with observed and sensitivity forcing data to study the under-ice water temperature evolution, revealing the cause, formation mechanism and impact of the warming phenomenon. The main conclusions are as follows.

During the period from the beginning of freezing to the complete melting of ice, the water temperature of Ngoring Lake continued to rise. The upper water temperature (2-10 m) was more than $T_{\rho,max}$, at highest 5.83 °C during 2015 to 2016, while the highest temperature in deep water was $T_{\rho,max}$.

Different with other tested models (Flake, and the lake scheme coupled in the CLM and WRF), LAKE2.3 could simulate the vertical thermal stratification during the ice-covered period in Ngoring Lake well, and the continuous rising of water temperature was simulated more accurately. Compared with MODIS surface temperature data, the *BIAS*, *RMSE* and *CC* were 1.42 °C, 3.25 °C and 0.96, respectively. The absolute values of *BIAS* and *RMSE* were less than 0.1 °C and 1 °C in 2 m, 9 m 14 m and 22 m. The *CC* of simulated and observed water temperature at 2 m, 9 m and 14 m were as high as 0.98, and the *CC* of simulated and observed water temperature at 22 m was 0.95.

Sensitivity simulations with perturbed local climate data showed that strong downward SR in TP played a dominant role in the water temperature rise during the ice-covered period in Ngoring Lake, and also the low precipitation played a positive feedback role. The smaller downward LR, lower air temperature and larger wind speed had negative feedback to the water temperature.

The sensitivity simulation results of the main physical parameters that affect the radiation transfer showed that with the increase of the albedo of ice, the rising trend of water temperature decreased and the length of the ice season increased. When albedo increased to 0.6, the lake water temperature no longer rose but tended to remain on a stable level. With the increase of extinction coefficient of ice, the increase of the temperature of the lake in the ice-covered period of Ngoring Lake decreased. The extinction coefficient of water had just a minor effect on water temperature under ice.

Compared with three more stable lake temperature profiles, the warming of Ngoring

https://doi.org/10.5194/tc-2021-398
Preprint. Discussion started: 14 February 2022

Lake ice-covered period caused the maximum sensible and latent heat releases after ice melting, and the difference of sensible and latent heat relesass lasted for 59-97 days between the lakes with the characteristics of three typical ice-covered periods which the water temperature remained fixed in each layer or was less than or equal to the maximum density temperature and Ngoring Lake. The distribution of water temperature affected the heat storage and heat transfer of lake surface after ice melting. The higher the water temperature, the higher the heat storage per unit area of the lake, and the greater were the sensible and latent heat release from the melting ice.

Data availability. The daily precipitation data from Chinese surface stations are available for purchase from the China Meteorological Data Service Center (CMDC, http://data.cma.cn/en/). The MODIS LST product are available from National Aeronautics and Space Administration (NASA) (https://earthdata.nasa.gov/). ERA5-Land data is available with funding from the European Union's Copernicus Climate Change Service (https://cds.climate.copernicus.eu/). Lake temperature data of Ngoring Lake in 2015 and 2016 were uploaded to Zenodo by Georgiy Kirillin (http://doi.org/10.5281/zenodo.4750910). The weather observation data of Ngoring Lake can be obtained from the website (https://nimbus.igb-berlin.de/index.php/s/Moqxgn29DbNFyr8).

Author contributions. MW and LW conceived the study. MW performed the modelling with contributions from VS, LW and ZL. YZ, RN and LY processed some data. MW, LW, ML and GK analyzed the model output. MW wrote the paper, with contributions from all co-authors.

Competing interests. The authors declare that they have no conflict of interest.

Acknowledgments. This study was supported by the National Key Research and Development Program of China (2019YFE0197600) and CAS "Light of West China" Program (E129030101, Y929641001). Victor Stepanenko was supported by Russian Ministry of Science and Higher Education, agreement No. 075-15-2019-1621.

References

Adrian, R., O'Reilly, C. M., Zagarese, H., Baines, S. B., Hessen, D. O., Keller, W., Livingstone, D. M., Sommaruga, R., Straile, D., Donk, E. V., Weyhenmeyer, G. A. and Winderl, M.: Lakes as sentinels of climate change, Limnol. Oceanogr., 54, 2283-2297, doi: 10.4319/ lo.2009.54.6_part_2.2283, 2009.

https://doi.org/10.5194/tc-2021-398
Preprint. Discussion started: 14 February 2022

Bai, Q. X., Li, R. L., Li, Z. J., Leppäranta, M., Arvola, L. and Li, M.: Time-series analyses of water temperature and dissolved oxygen concentration in Lake Valkea-Kotinen (Finland) during ice season, Ecol Inform, 36, 181-189, doi: 10.1016/j.ecoinf.2015.06.009, 2016.

Cao X. W., Lu P., Leppäranta M., Arvola L., Huotari J., Shi X H., Li G. Y. and Li Z. J.: Solar radiation transfer for an ice-covered lake in the central Asian arid climate zone, Inland Waters, 11, 89-103, doi: 10.1080/20442041.2020.1790274, 2020.

Bruesewitz, D. A., Carey, C. C., Richardson, D. C. and Weathers, K. C.: Under-ice thermal stratification dynamics of a large, deep lake revealed by high-frequency data, Limnol. Oceanogr., 60, 347-359, doi: 10.1002/lno.10014, 2015.

Chen, Z., Wang, X. Z., Lv, H., Lu, T. Y., Wan, Z. W. and Wang, W.: Observational multi-time Scales temporal variations in water temperature of Lake Taihu and its influencing factors, Science Technology and Engineering, 21, 4793-4800, doi: CNKI:SUN:KXJS.0.2021-12-008, 2021.

Dai, Y. J., Wei, N., Huang, A. N., Zhu S. G., Shangguan. W., Yuan, H., Zhang S. P. and Liu, S. F.: The lake scheme of the Common Land Model and its performance evaluation (in Chinese), Chin Sci Bull, 63, 3002-3021, doi: 10.1360/n972018-00609, 2018.

Dokulil, M. T.: Predicting summer surface water temperatures for large Austrian lakes in 2050 under climate change scenarios, Hydrobiologia, 731, 19-29, doi: 10.1007/s10750-013-1550-5, 2013.

Donlon, C. J., Minnett, P. J., Gentemann, C., Nightingale, T. J., Barton, I. J., Ward, B., and Murray, M. J.: Toward Improved Validation of Satellite Sea Surface Skin Temperature Measurements for Climate Research, J. Clim., 15, 353–369, doi: 10.1175/15200442(2002)015<0353:TIVOSS>2.0.CO;2, 2002.

Duan, A. M. and Xiao, Z. X.: Does the climate warming hiatus exist over the Tibetan Plateau?, Sci. Rep., 5, 1-9, doi: 10.1038/srep13711, 2015.

Efremova, T., Palshin, N. and Zdorovennov, R.: Long-term characteristics of ice phenology in Karelian lakes, EST J EARTH SCI, 62, 33-41, doi: 10.3176/earth.2013.04, 2013.

Erm, A., Jakkila, J., Lei, R. B., Jaatinen, E. and Lepparanta, M.: Ice Cover Optical Properties of some Finnish and Estonian Lakes, 20th IAHR International Symposium on Ice, 1-13, 2010.

Fang, N., Yang, K., Lazhu, Chen, Y. Y., Wang, J. B. and Zhu, L. P.: Research on the application of WRF-lake Modeling at Nam Co Lake on the Qinghai-Tibetan Plateau, Plateau Meteorology, 36, 610-618, doi: 10.7522/j.issn.1000-0534.2016.00038, 2017.

Fang, X. and Stefan, H. G.: Long-term lake water tem- perature and ice cover simulations_measurements, Cold Reg Sci Technol, 24, 289-304, 1996.

Gan, G. J. and Liu, Y. B.: Heat Storage Effect on Evaporation Estimates of China's

https://doi.org/10.5194/tc-2021-398
Preprint. Discussion started: 14 February 2022

Largest Freshwater Lake, J. Geophys, 125, 1-14, doi: 10.1029/2019jd032334, 2020.

Gerken, T., Biermann, T., Babel, W., Herzog, M., Ma, Y., Foken, T. and Graf, H.-F.: A modelling investigation into lake-breeze development and convection triggering in the Nam Co Lake basin, Tibetan Plateau, Theor. Appl. Climatol., 117, 149-167, doi: 10.1007/s00704-013-0987-9, 2013.

Guseva, S., Stepanenko, V., Shurpali, N., Biasi, C., Marushchak, M. E. and Lind, S. E.: Numerical Simulation of Methane Emission from Subarctic Lake in Komi Republic (Russia), Geography, Environment, Sustainability, 9, 58-74, doi: 10.15356/2071-9388_02v09_2016_05, 2016.

Hardenbicker, P., Viergutz, C., Becker, A., Kirchesch, V., Nilson, E. and Fischer, H.: Water temperature increases in the river Rhine in response to climate change, Reg Environ Change, 17, 299-308, doi: 10.1007/s10113-016-1006-3, 2016.

Heiskanen, J. J., Mammarella, I., Ojala, A., Stepanenko, V., Erkkilä, K. M., Miettinen, H., Sandström, H., Eugster, W., Leppäranta, M., Järvinen, H., Vesala, T. and Nordbo, A.: Effects of water clarity on lake stratification and lake-atmosphere heat exchange, J. Geophys, 120, 7412-7428, doi: 10.1002/2014jd022938, 2015.

Hersbach, H., Bell, B., Berrisford, P., Hirahara, S., Horányi, A., Muñoz-Sabater, J., Nicolas, J., Peubey, C., Radu, R., Schepers, D., Simmons, A., Soci, C., Abdalla, S., Abellan, X., Balsamo, G., Bechtold, P., Biavati, G., Bidlot, J., Bonavita, M., Chiara, G., Dahlgren, P., Dee, D., Diamantakis, M., Dragani, R., Flemming, J., Forbes, R., Fuentes, M., Geer, A., Haimberger, L., Healy, S., Hogan, R. J., Hólm, E., Janisková, M., Keeley, S., Laloyaux, P., Lopez, P., Lupu, C., Radnoti, G., Rosnay, P., Rozum, I., Vamborg, F., Villaume, S. and Thépaut, J. N.: The ERA5 global reanalysis, Quarterly Journal of the Royal Meteorological Society, Q J R Meteorol Soc, 146, 1999-2049, doi: 10.1002/qj.3803, 2020.

Huang, A. N., Lazhu, Wang, J. B., Dai, Y. J., Yang, K., Wei, N., Wen, L. J., Wu, Y., Zhu, X. Y., Zhang, X. D. and Cai, S. X.: Evaluating and Improving the Performance of Three 1-D Lake Models in a Large Deep Lake of the Central Tibetan Plateau, J. Geophys, 124, 3143-3167, doi: 10.1029/2018JD029610, 2019.

Immerzeel, W. W., Beek, L. P. H. and Bierkens, M. F. P.: Climate change will affect the Asian Water Towers, J Glaciol, 328, 1382-1385, doi: 10.1126/science.1187443, 2010.

Jiang, J. C., Liu, J. Z., Qin, C. Z., Miu, Y. M. and Zhu A. X.: Near-surface air temperature lapse rates and seasonal and type differences in China, Progress in Geography, 35, 1538-1548, doi: 10.18306/dlkxjz.2016.12.010, 2016.

Kirillin, G. B., Shatwell, T. and Wen, L. J.: Ice-covered lakes of Tibetan Plateau as solar heat collectors, Geophys. Res. Lett., 48, 1-12, doi: 10.1029/2021gl093429, 2021.

Lazhu, Yang, K., Hou, J. Z., Wang, J. B., Lei, Y. B., Zhu, L. P., Chen, Y. Y., Wang, M. D. and He, X. G.: A new finding on the prevalence of rapid water warming durinig lake ice melting on the Tibetan Plateau, Sci. Bull., 66, 2358-2361, doi: 10.1016/j.scib.2021.07.022, 2021.

Lazhu, Yang, K., Wang, J. B., Lei, Y. B., Chen, Y. Y., Zhu, L. P., Ding, B. H. and Qin, J.: Quantifying evaporation and its decadal change for Lake Nam Co, central Tibetan Plateau, J. Geophys, 121, 7578-7591, doi: 10.1002/2015jd024523, 2016.

Lei, R. B., Leppäranta, M., Erm, A., Jaatinen, E. and Pärn, O.: Field investigations of apparent optical properties of ice cover in Finnish and Estonian lakes in winter 2009, EST J EARTH SCI, 60, 50-64, doi: 10.3176/earth.2011.1.05, 2011.

Leppäranta, M.: Freezing of Lakes and the Evolution of Their ice Cover, Germany: Springer Science & Business Media, 2014.

Li, G. C., Liu, Z. G., Zhang, M., Li, J., Pi, K., Xiong, Y. and Xu, J.: A preliminary study of effects of warming on the nutrients dynamic in sediment of hypereutrophic shallow lake, Acta Ecologica Sinica, 35, 4016-4025, doi: 10.5846/stxb201309102244, 2015a.

Li, Z. G., Ao, Y. H., Lyu, S. H., Lang, J. H., Wen, L. J., Stepanenko, V., Meng, X. H. and Zhao, L.: Investigation of the ice surface albedo in the Tibetan Plateau lakes based on the field observation and MODIS products, J Glaciol, 64, 506-516, doi: 10.1017/jog.2018.35, 2018.

Li, Z. G., Lv, S. H., Wen, L. J., Ao, Y. H., Zhao, L. and Zhang, S. B.: Influence of incursion of dry cold air on atmospheric boundary layer process in Ngoring Lake Basin, Plateau Meteorology, 35, 1200-1211, doi: 10.7522/j.issn.1000-0534.2015.00076, 2016a.

Li, Z. G., Lyu, S. H., Ao, Y. H., Wen, L. J., Zhao, L. and Wang, S. Y.: Long-term energy flux and radiation balance observations over Lake Ngoring, Tibetan Plateau, Atmos Res, 155, 13-25, doi: 10.1016/j.atmosres.2014.11.019, 2015b.

Li, Z. G., Lyu, S. H., Wen, L. J., Zhao, L., Ao, Y. H. and Meng, X. H.: Study of freeze-thaw cycle and key radiation transfer parameters in a Tibetan Plateau lake using LAKE2.0 model and field observations, J Glaciol, 45, 1-16, doi: 10.1017/jog.2020.87, 2020.

Li, Z. J., Bai, Y. L., Li, H. Y., Arvola, L. and Lepparanta, M.: Understanding the Dissolved Oxygen Concentration under Ice in Lake Valkea-Kotinen (Finland): Data Analysis, 23rd IAHR International Symposium on Ice, 1-8, 2016b.

Muñoz-Sabater, J., Dutra, E., Agustí-Panareda, A., Albergel, C., Arduini, G., Balsamo, G., Boussetta, S., Choulga, M., Harrigan, S., Hersbach, H., Martens, B., Miralles, D. G., Piles, M., Rodríguez-Fernández, N. J., Zsoter, E., Buontempo, C. and Thépaut, J.-N.: ERA5-Land: A state-of-the art global reanalysis dataset for land applications, Earth Syst. Sci. Data, 1-50, doi: 10.5194/essd-2021-82, 2021.

Nordbo, A., Launiainen, S., Mammarella, I., Leppäranta, M., Huotari, J., Ojala, A. and Vesala, T.: Long-term energy flux measurements and energy balance over a small boreal lake using eddy covariance technique, J. Geophys, 116, 1-17, doi: 10.1029/2010jd014542, 2011.

O'Reilly, C. M., Sharma, S., Gray, D. K., Hampton, S. E., Read, J. S., Rowley, R. J., Schneider, P., Lenters, J. D., McIntyre, P. B., Kraemer, B. M., Weyhenmeyer, G. A., Straile, D., Dong, B., Adrian, R., Allan, M. G., Anneville, O., Arvola, L., Austin, J., Bailey, J. L., Baron, J. S., Brookes, J. D., Eyto, E., Dokulil, M. T., Hamilton, D. P., Havens, K., Hetherington, A. L., Higgins, S. N., Hook, S., Izmest'eva, L. R., Joehnk, K. D., Kangur, K., Kasprzak, P., Kumagai, M., Kuusisto, E., Leshkevich, G., Livingstone, D. M., MacIntyre, S., May, L., Melack, J. M., Mueller-Navarra, D. C., Naumenko, M., Noges, P., Noges, T., North, R. P., Plisnier, P. D., Rigosi, A., Rimmer, A., Rogora, M., Rudstam, L. G., Rusak, J. A., Salmaso, N., Samal, N. R., Schindler, D. E., Schladow, S. G., Schmid, M., Schmidt, S. R., Silow, E., Soylu, M. E., Teubner, K., Verburg, P., Voutilainen, A., Watkinson, A., Williamson, C. E. and Zhang, G.: Rapid and highly variable warming of lake surface waters around the globe, Geophys. Res. Lett., 42, 1-9, doi: 10.1002/2015gl066235, 2015.

Perovich, D. K. and Polashenski, C.: Albedo evolution of seasonal Arctic sea ice, Geophys. Res. Lett., 39, 1-6, doi: 10.1029/2012gl051432, 2012.

Qin, B. Q., Zhu, G. W., Gao, G., Zhang, Y. L., Li, W., Paerl, H. W. and Carmichael, W. W.: A drinking water crisis in Lake Taihu, China: linkage to climatic variability and lake management, J. Environ. Manage., 45, 105-112, doi: 10.1007/s00267-009-9393-6, 2009.

Ramp, C., Delarue, J., Palsboll, P. J., Sears, R. and Hammond, P. S.: Adapting to a warmer ocean--seasonal shift of baleen whale movements over three decades, PLoS One, 10, 1-15, doi: 10.1371/journal.pone.0121374, 2015.

Rösner, R. R., Müller-Navarra, D. C. and Zorita, E.: Trend analysis of weekly temperatures and oxygen concentrations during summer stratification in Lake Plußsee: A long-term study, Limnol. Oceanogr., 57, 1479-1491, doi: 10.4319/lo.2012.57.5.1479, 2012.

Saloranta, T. M., Forsius, M., Järvinen, M. and Arvola, L.: Impacts of projected climate change on the thermodynamics of a shallow and a deep lake in Finland: model simulations and Bayesian uncertainty analysis, HYDROL RES, 40, 234-248, doi: 10.2166/nh.2009.030, 2009.

Schmid, M., Hunziker, S. and Wüest, A.: Lake surface temperatures in a changing climate: a global sensitivity analysis, Clim Change, 124, 301-315, doi: 10.1007/s10584-014-1087-2, 2014.

Shang, Y. X., Song, K. S., Jiang, P., Ma, J. H., Wen, Z. D. and Zhao, Y.: Optical absorption properties and diffuse attenuation of photosynthetic active radiation for inland waters across the Tibetan Plateau, Journal of Lake Sciences, 30, 802-811, doi:

10. 18307 /2018. 0322, 2018.
Sharma, S., Gray, D. K., Read, J. S., O'Reilly, C. M., Schneider, P., Qudrat, A., Gries, C., Stefanoff, S., Hampton, S. E., Hook, S., Lenters, J. D., Livingstone, D. M., McIntyre, P. B., Adrian, R., Allan, M. G., Anneville, O., Arvola, L., Austin, J., Bailey, J., Baron, J. S., Brookes, J., Chen, Y., Daly, R., Dokulil, M., Dong, B., Ewing, K., de Eyto, E., Hamilton, D., Havens, K., Haydon, S., Hetzenauer, H., Heneberry, J., Hetherington, A. L., Higgins, S. N., Hixson, E., Izmest'eva, L. R., Jones, B. M., Kangur, K., Kasprzak, P., Koster, O., Kraemer, B. M., Kumagai, M., Kuusisto, E., Leshkevich, G., May, L., MacIntyre, S., Muller-Navarra, D., Naumenko, M., Noges, P., Noges, T., Niederhauser, P., North, R. P., Paterson, A. M., Plisnier, P. D., Rigosi, A., Rimmer, A., Rogora, M., Rudstam, L., Rusak, J. A., Salmaso, N., Samal, N. R., Schindler, D. E., Schladow, G., Schmidt, S. R., Schultz, T., Silow, E. A., Straile, D., Teubner, K., Verburg, P., Voutilainen, A., Watkinson, A., Weyhenmeyer, G. A., Williamson, C. E. and Woo, K. H.: A global database of lake surface temperatures collected by in situ and satellite methods from 1985-2009, Sci. Data, 2, 1-19, doi: 10.1038/sdata.2015.8, 2015.
Song, C. Q., Huang, B. and Ke, L. H.: Modeling and analysis of lake water storage changes on the Tibetan Plateau using multi-mission satellite data, Remote Sens Environ, 135, 25-35, doi: 10.1016/j.rse.2013.03.013, 2013.
Song, X. Y., Wen, L. J., Li, M. S., Du, J., Su, D. S., Yin, S. C. and Lv, Z.: Comparative Study on Applicability of Different Lake Models to Typical Lakes in Qinghai-Tibetan Plateau, Plateau Meteorology, 39, 213-225, doi: 10.7522/j.issn.1000-0534.2019.00102, 2020.
Stepanenko, V., Mammarella, I., Ojala, A., Miettinen, H., Lykosov, V. and Vesala, T.: LAKE 2.0: a model for temperature, methane, carbon dioxide and oxygen dynamics in lakes, Geosci Model Dev, 9, 1977-2006, doi: 10.5194/gmd-9-1977-2016, 2016.
Stepanenko, V. M. and Lykossov, V. N.: Numerical modeling of heat and moisture transfer processes in a system lake soil, Russ. Meteorol. Hydrol., 3, 95-104, doi: 2005.
Stepanenko, V. M., Machul'skaya, E. E., Glagolev, M. V. and Lykossov, V. N.: Numerical modeling of methane emissions from lakes in the permafrost zone, IZV ATMOS OCEAN PHY+, 47, 252-264, doi: 10.1134/s0001433811020113, 2011.
Stepanenko, V. M., Repina, I. A., Ganbat, G. and Davaa, G.: Numerical Simulation of Ice Cover of Saline Lakes, IZV ATMOS OCEAN PHY+, 55, 129-138, doi: 10.1134/s0001433819010092, 2019.
Su, R. M. Z., Ma, W. Q., M, Y. M., Xie, Z. P., Wang, B. B., Hu, W. and Liu, J. S.: Investigation of thermal stratification and mixed layer depth in La'ang Co in the Tibetan Plateau*, Journal of Lake Sciences, 33, 550-560, doi: 10. 18307 /2021. 0220, 2021.
Tavares, M., Cunha, A., Motta-Marques, D., Ruhoff, A., Cavalcanti, J., Fragoso, C., Martín Bravo, J., Munar, A., Fan, F. and Rodrigues, L.: Comparison of Methods to

https://doi.org/10.5194/tc-2021-398
Preprint. Discussion started: 14 February 2022

The Cryosphere Discussions

Estimate Lake-Surface-Water Temperature Using Landsat 7 ETM+ and MODIS Imagery: Case Study of a Large Shallow Subtropical Lake in Southern Brazil, Water, 11, 1-21, doi: 10.3390/w11010168, 2019.

Thiery, W. I. M., Stepanenko, V. M., Fang, X., Jöhnk, K. D., Li, Z., Martynov, A., Perroud, M., Subin, Z. M., Darchambeau, F., Mironov, D. and Van Lipzig, N. P. M.: LakeMIP Kivu: evaluating the representation of a large, deep tropical lake by a set of one-dimensional lake models, Tellus A, 66, 1-18, doi: 10.3402/tellusa.v66.21390, 2014.

Tolonen, A.: Application of a bioenergetics model for analysis of growth and food consumption of subarctic whitefish Coregonus lavaretus (L.) in Lake Kilpisjärvi, Finnish Lapland, Hydrobiologia, 390, 153–169, doi: 10.1023/A:1003525008870, 1998, 1998.

Wan, W., Long, D., Hong, Y., Ma, Y. Z., Yuan, Y., Xiao, P. F., Duan, H. T., Han, Z. Y. and Gu, X. F.: A lake data set for the Tibetan Plateau from the 1960s, 2005, and 2014, Sci. Data, 3, 1-13, doi: 10.1038/sdata.2016.39, 2016.

Wan, Z., Zhang, Y., Zhang, Q. and Li, Z. L.: Quality assessment and validation of the MODIS global land surface temperature, Int J Remote Sens, 25, 261-274, doi: 10.1080/0143116031000116417, 2004.

Wang, M. D., Hou, J. Z. and Lei, Y. B.: Classification of Tibetan lakes based on variations in seasonal lake water temperature, Chinese Science Bulletin, 59, 4847-4855, doi: 10.1007/s11434-014-0588-8, 2014.

Wang, M. X., Wen, L. J., Li, Z. G. and Su, D. S.: Study on the Warming Characteristics during the Ice-covered Period of Ngoring Lake in the Qinghai-Xizang Plateau, Plateau Meteorology, 40, 965-976, doi: 10. 7522/j. issn. 1000-0534. 2020. 00112, 2021.

Weitere, M., Vohmann, A., Schulz, N., Linn, C., Dietrich, D. and Arndt, H.: Linking environmental warming to the fitness of the invasive clamCorbicula fluminea, Glob Chang Biol, 15, 2838-2851, doi: 10.1111/j.1365-2486.2009.01925.x, 2010.

Wen, L. J., Lv, S. H., Li, Z. G., Zhao, L. and Nagabhatla, N.: Impacts of the Two Biggest Lakes on Local Temperature and Precipitation in the Yellow River Source Region of the Tibetan Plateau, Adv. Meteorol., 2015, 1-10, doi: 10.1155/2015/248031, 2015.

Wen, L. J., Lyu, S. H., Kirillin, G., Li, Z. G. and Zhao, L.: Air–lake boundary layer and performance of a simple lake parameterization scheme over the Tibetan highlands, Tellus A, 68, 1-15, doi: 10.3402/tellusa.v68.31091, 2016.

Wu, Y., Huang, A. N., Lazhu, Yang, X. Y., Qiu, B., Zhang, Z., Q. and Zhang X., D.: Numerical Study of the Thermal Structure and Circulation in a Large and Deep Dimictic Lake Over Tibetan Plateau, J. Geophys, 126, 1-22, doi: 10.1029/2021jc017517, 2021.

Xu, L. J. and Liu, H. Z.: Numerical Simulation of the lake effect of Erhai in the Yunnan-Guizhou Plateau area, Acta Meteorol. Sin., 73, 789-802, doi: 10.11676/qxxb2015.047, 2015.

Yang, B., Wells, M. G., McMeans, B. C., Dugan, H. A., Rusak, J. A., Weyhenmeyer, G. A., Brentrup, J. A., Hrycik, A. R., Laas, A., Pilla, R. M., Austin, J. A., Blanchfield, P. J., Carey, C. C., Guzzo, M. M., Lottig, N. R., MacKay, M. D., Middel, T. A., Pierson, D. C., Wang, J. and Young, J. D.: A New Thermal Categorization of Ice-Covered Lakes, Geophys. Res. Lett., 48, 1-11, doi: 10.1029/2020gl091374, 2021.

Yang, B., Young, J., Brown, L. and Wells, M.: High-Frequency Observations of Temperature and Dissolved Oxygen Reveal Under-Ice Convection in a Large Lake, Geophys. Res. Lett., 44, 12218-12226, doi: 10.1002/2017gl075373, 2017.

Yang, K., Wu, H., Qin, J., Lin, C. G., Tang, W. J. and Chen, Y. Y.: Recent climate changes over the Tibetan Plateau and their impacts on energy and water cycle: A review, Glob Planet Change, 112, 79-91, doi: 10.1016/j.gloplacha.2013.12.001, 2014.

Yang, X. Y. and Wen, J.: Numberical Simulation of Characteristic of Atmospheric Boundary Layer over Lake Gyaring and Ngoring, Plateau Meteorology, 31, 927-934, doi: 2012.

Zhang, G. Q., Luo, W., Chen, W. F. and Zheng, G. X.: A robust but variable lake expansion on the Tibetan Plateau, Sci. Bull., 64, 1306-1309, doi: 10.1016/j.scib.2019.07.018, 2019.

Zhang, G. Q., Yao, T. D., Xie, H. J., Qin, J., Ye, Q. H., Dai, Y. F. and Guo, R. F.: Estimating surface temperature changes of lakes in the Tibetan Plateau using MODIS LST data, J. Geophys, 119, 8552-8567, doi: 10.1002/2014jd021615, 2014.

Zhang, H., Shan, B. Q., Ao, L., Tang, W. Z. and Wen, S. F.: Past atmospheric trace metal deposition in a remote lake (Lake Ngoring) at the headwater areas of Yellow River, Tibetan Plateau, Environ. Earth Sci., 72, 399-406, doi: 10.1007/s12665-013-2960-4, 2013.

Zhu, L. P., Peng , P., Zhang, G. Q., Qiao, B. J., Liu, C., Yang, R. M. and Wang, J. B.: The role of Tibetan Plateau lakes in surface water cycle under global changes, Journal of Lake Sciences, 32, 597-608, doi: 10.18307/2020.0301, 2020.

Zolfaghari, K., Duguay, C. R. and Kheyrollah Pour, H.: Satellite-Derived Light Extinction Coefficient and its Impact on Thermal Structure Simulations in a 1-D Lake Model, Hydrol Earth Syst Sci, 1-36, doi: 10.5194/hess-2016-82, 2017.